

**A GLOBAL DEGREE AND ORDER 1200 MODEL OF THE LUNAR GRAVITY FIELD USING GRAIL MISSION DATA.** Sander Goossens<sup>1,2</sup>, Frank G. Lemoine<sup>2</sup>, Terence J. Sabaka<sup>2</sup>, Joseph B. Nicholas<sup>2,3</sup>, Erwan Mazarico<sup>2</sup>, David D. Rowlands<sup>2</sup>, Bryant D. Loomis<sup>2,5</sup>, Douglas S. Chinn<sup>2,5</sup>, Gregory A. Neumann<sup>2</sup>, David E. Smith<sup>4</sup>, Maria T. Zuber<sup>4</sup>. <sup>1</sup>Center for Research and Exploration in Space Science and Technology, University of Maryland Baltimore County, 1000 Hilltop Circle, Baltimore MD 21250 U.S.A. (email: [sander.j.goossens@nasa.gov](mailto:sander.j.goossens@nasa.gov)), <sup>2</sup>NASA GSFC, Code 698, 8800 Greenbelt Road, Greenbelt MD 20771 U.S.A.; <sup>3</sup>Emergent Space Technologies, 6411 Ivy Lane, Greenbelt, MD 20770, U.S.A.; <sup>4</sup>Massachusetts Institute of Technology, 77 Massachusetts Avenue, Cambridge MA 02139 USA; <sup>5</sup>Stinger Ghaffarian Technologies, 7701 Greenbelt Road, Greenbelt, MD 20770 U.S.A.

**Introduction:** The primary science objectives of the Gravity Recovery and Interior Laboratory (GRAIL) mission are to determine the structure of the lunar interior from crust to core and to advance the understanding of the thermal evolution of the Moon [1,2]. These objectives are to be achieved by producing a high-quality, high-resolution map of the gravitational field of the Moon. The concept of the GRAIL mission and its measurements is based on the successful GRACE mission which is mapping the gravity field of the Earth [3]: the distance between two co-orbiting spacecraft was measured precisely using a Ka-band ranging system [4], augmented by tracking from Earth using the Deep Space Network [5].

The GRAIL mission consisted of two separate phases: a primary mission phase, which lasted from March 1, 2012 until May 29, 2012, where the spacecraft were at an average altitude of 50 km above lunar surface, and an extended mission phase, which lasted from August 30, 2012, until December 14, 2012, during which the average spacecraft altitude was 23 km. In the latter part of the extended mission this altitude was lowered further to 20 km (November 18) and finally 11 km (December 6). Two different analysis groups have processed the GRAIL data: one at the Jet Propulsion Laboratory (JPL) [6,7], and one at NASA's Goddard Space Flight Center (GSFC) [8,9]. Here, we present the latest global model developed by the GSFC group, a model of degree and order 1200 in spherical harmonics (equivalent block size of 4.5 km by 4.5 km at the lunar equator).

**Methods:** We analyzed the GRAIL data using our GEODYN II software [10]. The data are divided into continuous spans of time called arcs, which are about 2.5 days long and centered around angular momentum desaturation events. We numerically integrate the equations of motion for both satellites simultaneously, using high-precision, high-fidelity models of the forces acting on the spacecraft and of the measurements. The force models used include a lunar gravity field model, degree-2 potential Love numbers  $k_{2m}$ , third-body perturbations of the Sun and planets, and solar and indirect (planetary) radiation pressure. We also forward-model the effects of dissipation in the Moon because

this changes the gravitational potential [11]. The measurement modeling uses high-precision corrections for relativity, station motion, and troposphere and ionosphere-induced media delays. We then compare computed measurements with the actual measurements, and use a least squares batch estimation approach [12] to adjust parameters describing the forces and measurements.

We conveniently divide the adjusted parameters into arc parameters (parameters that only influence the measurements within a certain arc, such as initial states for the spacecraft) and common parameters (parameters that affect all measurements, such as the coefficients of the spherical harmonic expansion of the gravitational potential). Our arc parameters include the initial states (position and velocity) of both satellites, and empirical accelerations. We include constant accelerations and accelerations with a period of one orbital revolution, in the radial, along-track and cross-track directions. We estimate such a set per satellite every quarter orbit, and we apply time-correlation to ensure smooth transitions between periods [13]. Our common parameters include the spherical coefficients for a degree and order 1200 model,  $k_{2m}$  Love numbers, the lunar gravitational parameter  $GM$ , and a scale factor for the forward model of interior dissipation [11].

The data used in our processing are 2-way S-band tracking data from the DSN, and the precise KBRR data. We weigh the DSN data at 0.12 mm/s (close to its expected noise level of 0.1 mm/s). KBRR data for the primary mission are weighted at 0.03 micron/s, and those for the extended mission at 0.05 micron/s. DSN data has a sample time of 10 s, that of primary mission KBRR data is 5 s, and that of extended mission KBRR data is 2 s.

Solar radiation pressure is one of the main forces acting on the GRAIL satellites. Early in the mission it was realized that the timing of eclipses was especially important, since a mismatch could introduce a signal of several tenths of microns/s into the KBRR residuals [13]. Despite careful modeling, there were still periods during which the eclipse timing was slightly off in our processing, which resulted in high KBRR residuals in localized areas at the selenocentric locations of eclipse

transitions. A careful re-analysis of the eclipse geometry, together with careful editing of the data, has improved the eclipse timings, resulting in an improved KBRR fit, particularly in the eclipse transition regions.

The high degree and order global models that we develop from the GRAIL data require the estimation of a large number of parameters. Our solution strategy is based on QR factorization [14], and at our current model resolution this is computationally intensive. We have therefore turned to using the supercomputers of the NASA Center for Climate Simulation (NCCS) at NASA/GSFC for the inversions.

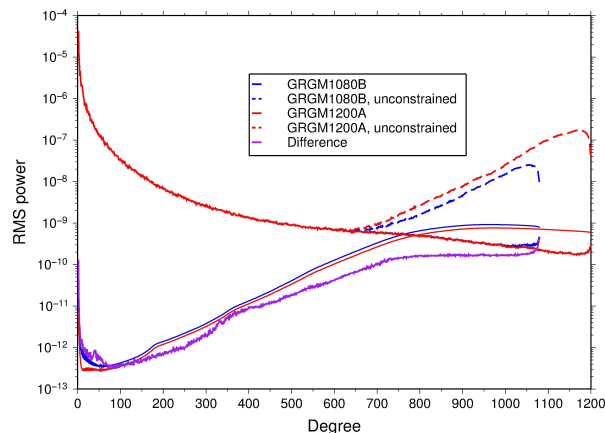


**Figure 1:** Power and error spectra for the GRGM1080B and GRGM1200A models. The power spectra show results for the constrained and unconstrained models. The RMS power for the coefficient differences between the models is also shown.

**Results:** We have processed all primary mission and extended mission data and determined a global model of degree and order 1200, named GRGM1200A. For this model, we used a Kaula rule of  $36 \times 10^{-5}/l^2$  for degrees  $l$  larger than 600. Figure 1 shows the power and error spectra of this solution, along with those of the GRGM1080B model, a degree and order 1080 solution that served as the starting model. The errors for the lower degrees for GRGM1200A have improved considerably, likely due to the use of radial accelerations. For both models shown in Figure 1, the error curves intersect the power curves. We stress that both models are calibrated in such a way that the formal residual statistics from the covariance matrix match the observed statistics, using a scaling factor derived from the square-root information filter [9,14]. This scaling factor was 1.79 for GRGM1080B, and it decreased to 1.64 for GRGM1200A, indicating more realistic formal errors for the new model. Model differences agree reasonably well with the scaled formal errors.

Figure 2 shows the correlations between gravity and gravity derived from topography (using Lunar

Orbiter Laser Altimeter, LOLA, data [15]). The new model GRGM1200A shows improvements over the GRGM1080B model, made clear in the inset of Figure 2 which zooms in on the degree range  $l=500-900$ .

The fit to the data also improve with the new model. Data fits for the late extended mission (December 2012, when the spacecraft were at their lowest altitudes over the lunar surface) are still higher than those for the rest of the mission, indicating that further improvements are possible. These will be pursued.

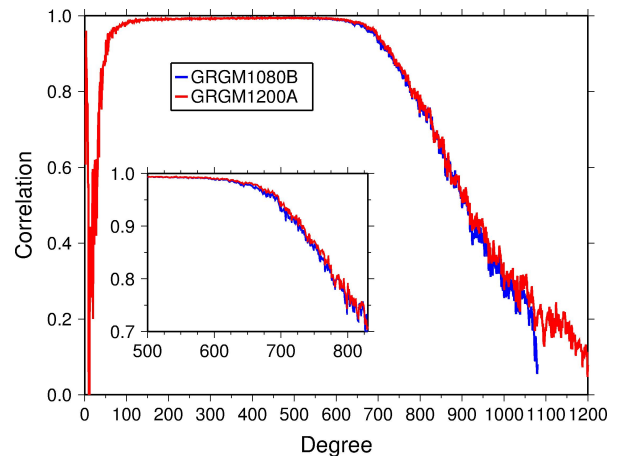


**Figure 2:** Correlations between gravity from LOLA-derived topography [15] and the GRGM1080B and GRGM1200A models.

**References:** [1] Zuber M. T. et al. (2012) *Science* doi: 10.1126/science.1231507. [2] Zuber M. T. et al. (2013) *Space Sci. Rev.* doi:10.1007/s11214-012-9952-7. [3] Tapley B. D. et al. (2004) *Science* doi:10.1126/science.1099192. [4] Klipstein et al. (2013) *Space Sci. Rev.* doi:10.1007/s11214-013-9973-x. [5] Asmar S.W. et al. (2013) *Space Sci. Rev.* doi: 10.1007/s11214-013-9962-0. [6] Konopliv A. S. et al. (2014) *Geophys. Res. Lett.* doi: 10.1002/2013GL059066. [7] Park R. S. et al. (2015) *AGU Fall Meeting*, paper G41B-01. [8] Lemoine F. G. et al. (2014) *Geophys. Res. Lett.*, doi: 10.1002/2014GL060027. [9] Lemoine F. G. et al. (2015) *AGU Fall Meeting*, paper P34A-06. [10] Pavlis D. E. et al. (2013) *GEODYN Operations Manual*. [11] Williams and Boggs (2015) *J. Geophys. Res. Planets*, doi:10.1002/2014JE004755. [12] Montenbruck O. and Gill E. (2000) *Satellite Orbits*, Springer-Verlag. [13] Lemoine F. G. et al. (2013) *J. Geophys. Res. Planets* 118, doi: 10.1002/jgre.20118. [14] Bierman G. J. (2006) *Factorization Methods*, Dover Publications. [15] Smith D. E. et al. (2010) *Geophys. Res. Lett.* 37, doi:10.1029/2010GL043751.